

# Moisture transfer of clothing-human body system during continuous sweating under radiant heat

Manhao Guan<sup>1,2</sup>, Simon Annaheim<sup>2</sup>, Martin Camenzind<sup>2</sup>, Jun Li<sup>1,3,4,\*</sup>, Sumit Mandal<sup>2</sup>, Agnes Psikuta<sup>2</sup>, René Michel Rossi<sup>2,\*</sup>

<sup>1</sup>College of Fashion and Design, Donghua University, 200051, Shanghai, China

<sup>2</sup>Empa, Swiss Federal Laboratories for Materials Science and Technology, Laboratory for Biomimetic Membranes and Textiles, CH-9014, St. Gallen, Switzerland

<sup>3</sup>Key Laboratory of Clothing Design and Technology, Donghua University, Ministry of Education, 200051, Shanghai, China

<sup>4</sup>Tongji University Shanghai Institute of Design and Innovation, Shanghai 200092, China

\*Corresponding authors: R.R. (email: [rene.rossi@empa.ch](mailto:rene.rossi@empa.ch)), J.L. (email: [lijun@dhu.edu.cn](mailto:lijun@dhu.edu.cn)).

## Abstract

Mass transfer due to perspired moisture in clothing system is critical for the understanding of thermo-physiology and thermal protection of clothed body. Previous studies usually investigated moisture transfer without considering the effect of liquid sweating or external heat hazards. To understand mechanisms of sweat evaporation, accumulation and dripping with continuous sweating under radiant heat, a multi-phase experiment was designed with a sweating Torso. The concept of clothed wettedness was proposed to understand sweat evaporation of clothed body. Results showed that the evaporation rate of clothed body increased with increasing perspiration rate and the rate increase can be explained by material properties which affected sweat accumulation ability (e.g., material composition, material hydrophilicity and evaporative resistance ( $R_{et}$ )). Results also demonstrated a dual relationship of  $R_{et}$  with the evaporation rate of clothed body. First, evaporation rate was increased for greater  $R_{et}$  due to the higher moisture accumulation. Second, when  $R_{et}$  exceeded a certain value, evaporation rate decreased with greater  $R_{et}$  due to the reduction in the mass transfer coefficient. For radiant heat exposure, evaporated sweat may condense on the skin surface, decreasing the evaporation rate and increasing the dripping rate. The sweat transfer process was also investigated in detail by the combined analysis of sweat transfer rate and evaporative cooling efficiency. The study provides insights into how continuous liquid sweat transfers and evaporates in clothed body and its interaction with clothing material and environment radiant heat, contributing to the understanding of thermo-physiological burden and thermal protection of clothed body with intensive activities.

## Key words

Sweat evaporation; clothed human body; sweat accumulation; radiant heat; steam burn; thermo-physiology.

## 1. Introduction

Firefighters and industrial workers wearing thermal protective clothing often perform intensive physical activities under radiant heat exposure, and consequently, sweat profusely. The perspired moisture is closely related to thermo-physiological responses but also affects the thermal protection of clothed human body. On one hand, the perspired moisture provides evaporative cooling to the body, relieving heat strain <sup>1</sup>. On the other hand, the liquid moisture can increase thermal conductivity and heat capacity of the clothing material, affecting skin burns when exposed to hazardous conditions <sup>2, 3</sup>. Therefore, the investigation of perspired moisture transfer of clothed human body in radiant heat provides helpful inputs to understand the thermo-physiological burden and thermal protection of protective clothing systems <sup>4</sup>.

<sup>5</sup>. The evaporation rate of clothing-body system is an important indicator of the moisture transfer process, providing information regarding thermal effects of perspired moisture. Previous research pointed out that the evaporation rate of perspired moisture depends on air velocity, the vapor pressure gradient between skin and ambient air and the vapor permeability of the clothing<sup>6, 7</sup>.

In early studies, the evaporation rate was usually quantified by human trials with the weight loss of (clothed) human body <sup>8-11</sup>. Sweat evaporative efficiency (the ratio of evaporative sweat to total sweat production) was introduced to understand the relationship between the evaporation rate and the sweat rate <sup>7, 12-14</sup>. Previous studies showed that sweat evaporative efficiency is related to skin wettedness. The efficiency could be unity when the skin wettedness is low and tends to decline when the wettedness increases <sup>7, 12, 15-19</sup>. Usually these studies investigated evaporation rate and sweat evaporative efficiency merely on nude subjects <sup>7, 15, 18</sup> or subjects with swimming trunks <sup>12</sup>. Some studies adopted the clothed human body, but without considering the effect of clothing material properties on the evaporation process <sup>16, 17</sup>.

Recently, the effect of clothing/material on the evaporation process is usually characterized by water vapor resistance (named as evaporative resistance in ASTM standards) through the sweating hot plate and thermal manikin measurements <sup>20-24</sup>. With lower water vapor resistance, the clothed body has a greater evaporation rate <sup>25</sup>. The existing experimental and model investigations of sweat evaporation usually assume that the sweat evaporates on the skin and only sweat vapor transfers through the clothing system<sup>26, 27</sup>. However, in practice, liquid sweat may transfer from the skin to the clothing layers and evaporate either from the skin or from the clothing.

Existing studies investigating the effect of liquid sweat usually adopted the pre-wetted skin and clothing. A human trial showed that the evaporative mass loss was greater with higher water content in the clothing<sup>9</sup>. The study conducted by Wang et al.'s showed that the evaporation rate was significantly lower when all the sweat was transferred to the clothing layer<sup>28</sup>. In Havenith et al.'s study<sup>25</sup>, they found that the evaporative mass loss reduced with decreased material vapor permeability, but showed no significant dependence on temperature nor any interaction of temperature and permeability, since the vapor pressure gradient between the skin and environment was held constant at the different temperatures. Their follow-up study<sup>29</sup> showed a clear reduction in evaporative mass loss with increasing clothing thickness. Cain and McLellan <sup>30</sup> explored the effect of liquid sweat on evaporation rate but without controlling sweat rate. Results showed that evaporation rate was greater when the fabric sample was in direct contact with the liquid surface. They hypothesized that the greater evaporation may result from a reduction of water vapor resistance of the material due to wicking of liquid sweat through fabric layers. Besides, a human trial study <sup>31</sup> showed that the hydrophilic clothing exhibited more favorable thermal physiological performance than the hydrophobic clothing, which indicates that material hydrophilicity may have effect on sweat evaporation.

In addition, in the field of thermal protective performance which considers external heat sources, the effect of liquid sweat was also usually simulated by pre-wetted materials. Through continuous recording of a balance, the evaporation rate of clothed manikin with pre-wetted inner clothing was calculated <sup>32</sup>. Results showed that radiant heat increased the evaporation rate of permeable clothing but had negligible effect on impermeable clothing. By means of thermocouple measurement techniques, a study investigated evaporation rate of pre-wetted materials under radiant heat exposure <sup>33</sup>. They found that the moisture location in the materials influenced the evaporation rate by affecting the temperature of the wet surface and the diffusion length. Except for these, most studies could not provide information on sweat transfer process due to technical limitations of measuring moisture transport <sup>33, 34</sup> and thus could not analyze how liquid and vaporous sweat transfer mechanisms affect heat transfer.

The aim of our study is to understand the sweat evaporation as well as the sweat accumulation and dripping of clothed human body with continuous sweating when exposed to radiant heat. By means of a clothed Torso manikin system, we obtained sweat evaporation rate, accumulation rate and dripping rate within a wide range of clothing materials. Three factors and their interaction influencing the evaporation process of the clothed human body were investigated: (I) the sweat rate; (II) the key material properties; (III) the external radiant heat. To further understand sweat transport within clothing, dynamic sweat transfer process was analyzed in detail. The study contributes to the understanding of liquid sweat transfer and its thermal effects in clothed human body, helping improve the thermal comfort and protection of human body.

## 2. Methods

### 2.1 Torso manikin

To accurately determine the sweat transfer<sup>1 35</sup> between the clothed human body and its surrounding environment, measurements were performed on a sweating thermal Torso (Fig. 1) (Swiss Federal Laboratories for Materials Science and Technology, St. Gallen, Switzerland)<sup>36, 37</sup>. The Torso consists of a multi-layered main cylinder with the dimension of an adult human Torso and two heated aluminum guards. The main cylinder can maintain a constant surface temperature by controlling heating power, simulating heat dissipation of human body. The two guards are used to prevent heat losses in the upward and downward directions. Fifty-four sweating outlets are evenly distributed over the surface of the main cylinder and are connected to internal, separately controlled valves to simulate various sweating levels. The balance system of the Torso consisting of three weighing scales was applied to measure the sweat transfer. Other detailed information regarding the Torso can be found in the literature<sup>38, 39</sup>.

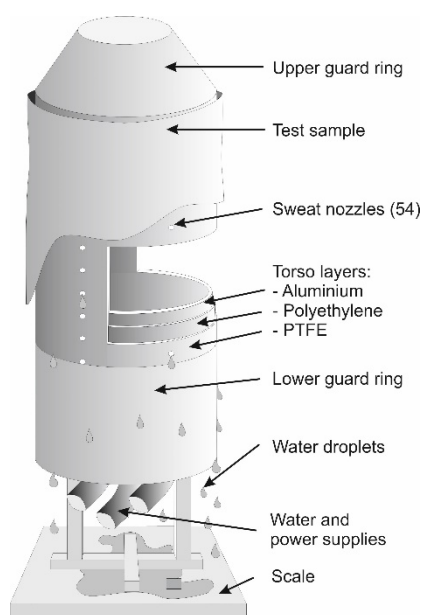


Fig. 1 Schematic diagram of the sweating thermal Torso. PTFE, polytetrafluoroethylene.

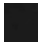
















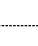



### 2.2 Clothing materials

Twelve common material systems of thermal protective clothing with different physical properties (Table 1) were selected, including seven single-layered materials of station uniforms (SU) and five multi-layered material systems of turnout gears (TG). As the research aim is to understand the transfer of liquid sweat,

<sup>1</sup> As the water is the main component ( $\approx 99\%$ ) of the sweat<sup>35</sup> and other minor components may complicate the heat and moisture transfer analyses, we used distilled water to simulate sweat in the current research stage. To emphasize the direction of the moisture source (i.e., sweat), we used the terminology “sweat” to refer to the sweat simulated by the torso system.

material hydrophilicity/hydrophobicity was included as a potential property influencing liquid sweat transfer. The hydrophilicity/hydrophobicity was defined by the contact angle of the innermost side of the tested material system. Each multi-layered material system was measured as a whole with the inside of inner layer facing to the water droplet. According to the measured contact angle, the pho-SU2, SU5, TG9 and TG10 were categorized as hydrophobic materials, while the other samples were categorized as hydrophilic materials. It should be noted that although the inside of inner layer of TG 9 and TG10 are hydrophobic, liquid water can still penetrate through the pores of the layer with contact pressure and accumulate within the material system. Besides, the radiation wavelength range of infrared lamps (SIC-CATHERM infra-red lamps, OSRAM Licht AG, Germany) used to simulate the external radiant heat was 590-2500 nm. Thus, material emissivity ( $\epsilon$ ) was also measured and averaged over this wavelength range.

**Table 1 Physical properties of clothing material systems**

Fabric Systems		Fiber Content	Color	Physical Properties*					
				Weight <sup>a</sup> (g/m2)	Thick- ness <sup>b</sup> (mm)	Contact angle <sup>c</sup> (°)	Thermal re- sistance ( $R_{ct}$ ) <sup>d</sup> (10- 3·°C·m2/W)	Evaporative resistance ( $R_{et}$ ) <sup>e</sup> (Pa·m2/W)	Emissiv- ity ( $\epsilon$ ) <sup>f</sup>
SU (single- layered material)	SU1	50% meta-aramid/50% fire retardant (FR) vis- cose		197.0	0.4	0	10.8	2.1	0.837
	phi- SU2	34% aramid/ 33% lyocell/ 31% modacrylic/ 2% anti-static fiber		241.6	0.6	0	13.4	2.7	0.648
	pho- SU2	34% aramid/ 33% lyocell/ 31% modacrylic/ 2% anti-static fiber		253.1	0.7	128.6	13.2	2.7	0.682
	SU3	93% meta-aramid/5% para-aramid/2% anti- static fiber		154.7	0.3	0	11.7	2.0	0.254
	SU4	93% meta-aramid/5% para-aramid/2% anti- static fiber		229.8	0.4	0	12.7	3.2	0.278
	SU5	55% FR Modacrylic/45% FR Cotton		367.3	0.7	130.7	16.6	3.4	0.247
	SU6	FR Cotton		366.8	0.8	0	14.5	4.4	0.421
TG (multi- layered material system)	TG7	99% aramid/1% beltron (OL) + PTFE coated meta-aramid (ML) + fleece (ML) + 50% meta- aramid/50% viscose (IL)	   	635.2	3.2	0	82.7	15.6	0.924
	TG8	Meta-aramid with thread on backside (OL) + PU liner on meta-aramid (ML) + aramid (IL)	  	592.1	3.8	0	95.4	23.9	0.933
	TG9	64% FR viscose/35% meta-aramid/1% antista- tic (OL, yellow) + PU coated 50% meta-ara- mid/50% FR viscose (ML) + 65% FR vi- scose/35% meta-aramid (IL)	  	587.8	2.0	130.8	46.6	9.4	0.489
	TG10	64% FR viscose/35% meta-aramid/1% antista- tic (OL, blue) + PTFE coated 50% meta-ara- mid/50% FR viscose (ML) + 65% FR vi- scose/35% meta-aramid (IL)	  	599.8	2.2	130.2	49.3	10.0	0.834
	TG11	Meta-aramid (OL) + PTFE coated 25% meta- aramid/25% para-ara- mid/50% basofil (ML) + non-woven meta-aramid quilted with 50% meta- aramid/50% FR viscose (IL)	  	493.0	2.3	0	71.0	16.8	0.901

For all turnout Gears, the images from top to bottom are the materials from the outermost layer to the innermost layer. \*Physical properties were measured according to <sup>a</sup>ISO 3801:1977 (by weighing balance of Mettler-Toledo, Switzerland), <sup>b</sup>ISO 5084:1996 (by thickness tester of Frank-PTI, Germany), <sup>c</sup>ASTM D7334 - 08(2013). If the contact angle of a material is 0°, it is categorized as hydrophilic. If the contact angle is greater than 90°, the material is categorized as hydrophobic, <sup>d</sup>intrinsic values, ISO 11092:2014 (by hot plate

tester of Hohenstein Institute, Germany) and <sup>b</sup>by extended FT-IR spectrometer VERTEX 80, Germany <sup>22, 40, 41</sup>. SU: station uniform; TG: turnout gear. OL: outer layer; ML: middle layer; IL: inner layer. PTFE: polytetrafluorethylene; PU: polyurethane.

## 2.3 Experiment design

### 2.3.1 Three-phase experiment

Experiments were performed in a climatic chamber with air temperature of  $20.0 \pm 0.5$  °C, relative humidity of  $50 \pm 2$  % and air velocity of  $0.65 \pm 0.10$  m/s. Before the experiments, clothing materials were preconditioned in the same chamber for at least 24 hours. To understand liquid sweat transfer in clothing system, the materials were wrapped on the Torso surface with direct contact.

The main experiment was designed to include three consecutive phases (Fig. 2) to simulate the fire-fighting scenario: preparatory work without sweating followed by sweating and finally additional radiant heat exposure when entering the fire field. The constant surface temperature mode of 35 °C was used to simulate the thermal state of human body according to ISO 18640<sup>36</sup>. In phase one (P1), the clothed Torso was kept in the dry thermal state for one hour. In phase two (P2), a pre-set sweat rate was applied for two hours. Three different sweat rates of 100, 175 and 250 g/h were chosen, corresponding to the sweat rate of 415.2-1038.1 g/h of a firefighter with low to moderate sweating level <sup>3</sup> (assuming a body surface area of 1.8 m<sup>2</sup> <sup>42</sup>). In phase three (P3), a 96x188 cm<sup>2</sup> radiant heat panel filled with the infrared lamps was used to expose the front side of the Torso to external radiant heat for another two hours, while the sweat rate was kept at its previous level. To guarantee the normal working of the Torso, the radiation intensity on the Torso surface was determined as 1 kW/m<sup>2</sup>, simulating the routine thermal environment for firefighters, in which the heat flux remains lower than 1.67 kW/m<sup>2</sup> <sup>43</sup>. Pre-tests with a thermal sensor (Schmidt-Boelter heat flux sensor, Medtherm Corporation, USA) were performed to identify a distance of 137 cm between the radiant heat panel and the front side of the Torso, to achieve the target radiation intensity. The test duration for each phase was determined according to the required time to reach the steady state of heat and moisture transfer.

Since the starting points of P2 and P3 of the main experiment contain different amounts of water in the clothing system, additional experiments were carried out similarly to the main experiment, but without radiant heat exposure during P3. This helped clarify that the different water content in the material had no significant effect on the moisture transfer results and differences in moisture transfer observed between P2 and P3 can be attributed to the effect of external radiant heat.

*P1: without radiation	*P2: without radiation	*P3: with radiation
Constant temperature: 35 °C; Without sweating; 1 hour	Constant temperature: 35 °C; Sweat rate: 100, 175, 250 g/h; 2 hours	Constant temperature: 35 °C; Sweat rate: 100, 175, 250 g/h; Radiation: 1 kW/m <sup>2</sup> ; 2 hours

Fig. 2 Schematic diagram of three-phase experiment.

### 2.3.2 Experimental measurement and calculation

#### (1) Sweat transfer

To evaluate the sweat transfer of the clothed Torso, the real-time sweat amount ( $m_{sweat}$ ) was controlled with weighing scale I (accuracy: 0.1 g, Mettler-Toledo SB8001, Mettler-Toledo GmbH, Greifensee, Switzerland); the real-time sweat accumulation ( $m_{accu}$ ) in the clothed Torso was obtained by the weight change of the clothed Torso (i.e.,  $m_{accu} = \Delta m_{clothed\ torso}$ ), measured by weighing scale II (accuracy: 1 g, Mettler-Toledo KCC150, Mettler-Toledo GmbH, Greifensee, Switzerland); the real-time dripping sweat was collected in a bottle and its weight ( $m_{drip}$ ) was measured by weighing scale III (accuracy: 0.1 g, Mettler-Toledo XS6001S, Mettler-Toledo GmbH, Greifensee, Switzerland). According to the relationship among the component weights of sweat transfer, the amount of evaporative sweat ( $m_{evap}$ ) can be obtained as eqn. (1).

$$m_{evap} = m_{sweat} - m_{accu} - m_{drip} \quad (1)$$

(a) Sweat transfer rate

The sweat rate ( $\dot{m}_{sweat}$ ), the evaporation rate ( $\dot{m}_{evap}$ ), the accumulation rate ( $\dot{m}_{accu}$ ) and the dripping rate ( $\dot{m}_{drip}$ ) were calculated as the slope of weight versus time during the steady state. Sweat evaporative efficiency ( $\eta_{evap}$ ), which is the ratio of the evaporative sweat to the total sweat production<sup>7, 12-14</sup>, was calculated according to eqn. (2).

$$\eta_{evap} = \frac{\dot{m}_{evap}}{\dot{m}_{sweat}} \quad (2)$$

(b) Sweat accumulation ability

For test cases with dripping sweat during the last 30 minutes of P2 and P3, the material tended to reach the maximum sweat accumulation amount. Thus, the sweat accumulation ability of the material can be calculated as the average value of the sweat accumulation amount in the clothed Torso during this period of time.

## (2) Vapor pressure gradient

To help understand the sweat transfer process, the vapor pressure gradient from the Torso surface to the environment was calculated based on the temperature and relative humidity measurements. At four sides (front, back, left and right side) of the clothed Torso, temperature and relative humidity underneath the clothing (on the Torso surface) and in the environment (next to the clothed Torso) were measured (MSR 145, MSR Electronics GmbH, Seuzach, Switzerland). MSR sensors were placed 8 cm below the upper edge of the Torso main cylinder.

### 2.3.3 Steady state criteria

Since the test condition was changed at the beginning of each phase, the heat and moisture transfer of the torso would change abruptly before reaching the steady state. The steady state in each phase was considered only, as the transient periods depended on inherent regulation properties of the methodology and, thus, may only provide limited information about moisture transfer behaviors. The steady state was determined by the Torso surface temperature, the heating power and the evaporation process. During the last 30 minutes of each phase, the coefficient of variation (CV) of the mean Torso surface temperature was less than 0.7 % and the CV of Torso heating power was less than 13.5 %. Compared to a previous study<sup>44</sup>, we considered that the heat transfer of the clothed Torso during this period of time reached the steady state. For each sweat rate, at least three replications of the materials were tested on the Torso, guaranteeing the CV of the Torso heating power among repetition tests to be less than 8.5 %. For all tests, the normalized root-mean-square deviation (NRMSD) of the evaporation rate ( $\dot{m}_{evap}$ ) during the last 30 minutes of P2 and P3 was lower than 1.1%, thus we considered that  $\dot{m}_{evap}$  was constant during this period of time and the evaporation process reached the steady state.

## 2.4 Theoretical analysis and concept of clothed wettedness

The evaporation rate from the nude skin of human body can be expressed as eqn. (3)<sup>6</sup>.  $\dot{m}_{sk}$  is the evaporation rate from the nude skin, g/h;  $A_{sk}$  is the skin area available for evaporation, m<sup>2</sup>;  $w_{sk}$  is the fraction of the body surface covered by water (skin wettedness), dimensionless;  $h_m$  is the mass transfer coefficient from the skin to the environment, g·m<sup>-2</sup>·h<sup>-1</sup>·kPa<sup>-1</sup>;  $P_{sk,s}$  and  $P_a$  are the saturated vapor pressure on the skin and the vapor pressure in the environment, kPa.

$$\dot{m}_{sk} = A_{sk} w_{sk} h_m (P_{sk,s} - P_a) \quad (3)$$

For the clothed human body, the evaporative mass loss from the body to the environment may occur both on the skin and within the clothing layers <sup>29</sup>. (Fig. 3). We assume that the clothing material is homogeneous, and the liquid water is distributed homogeneously in the material. We divided the clothing into  $n$  layers. Thus, for a certain layer  $k$  ( $k = 1, \dots, n$ ), the evaporation rate  $\dot{m}_{evap,k}$  can be written as eqn. (4).

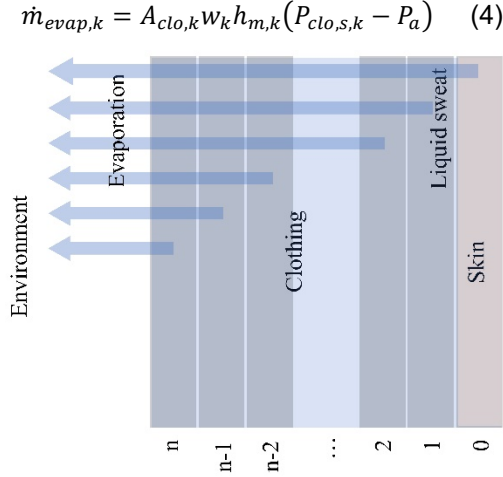


Fig. 3 Schematic diagram of evaporation of the liquid sweat in clothed human body.

To simplify the expression of the subsequent formulae, the skin layer is denoted by layer  $k = 0$ . Thus, for the whole skin and clothing system, the evaporation rate ( $\dot{m}_{evap}$ ) can be written as eqn. (5).

$$\dot{m}_{evap} = \sum_{k=0}^n A_{clo,k} w_k h_{m,k} (P_{clo,s,k} - P_a) \quad (5)$$

$A_{clo,k}$  ( $k = 0, \dots, n$ ) are the surface area of skin covered by clothing and the area of each clothing layer,  $m^2$ ; for a certain material system,  $A_{clo,k}$  is constant.

$w_k$  ( $k = 0, \dots, n$ ) are the wettedness of skin and each clothing layer, dimensionless. We also define  $w_{clo}$  as the wettedness for the whole clothing system.

$h_{m,k}$  ( $k = 0, \dots, n$ ) are the mass transfer coefficients from each layer to the environment,  $g \cdot m^{-2} \cdot h^{-1} \cdot kPa^{-1}$ , calculated as eqn. (6).  $R_{et}$  is material intrinsic evaporative resistance,  $kPa \cdot m^2 \cdot W^{-1}$ . According to literature <sup>30</sup>, due to wicking of liquid sweat through the material, there will be a reduction of evaporative resistance of the material. Based on this, we consider that the evaporative resistance of the wet material is the function of clothed wettedness  $w_{clo}$ , denoted as  $R_{et}(w_{clo})$ , and with greater  $w_{clo}$ ,  $R_{et}(w_{clo})$  decreases.  $R_{e,bl}$  is evaporative resistance of the boundary layer,  $kPa \cdot m^2 \cdot W^{-1}$ . Since in our study, the air velocity is constant,  $R_{et,bl}$  is constant.  $\lambda$  is the latent heat of sweat evaporation,  $0.673 W \cdot h \cdot g^{-1}$  at  $35^\circ C$ . Since  $R_{et}(w_{clo})$  decreases with greater  $w_{clo}$  and  $R_{et,bl}$  is constant,  $h_{m,k}(w_{clo})$  increases with greater  $w_{clo}$ .

$$h_{m,k}(w_{clo}) = \frac{1}{(R_{et}(w_{clo}) \times \frac{n-k}{n} + R_{et,bl}) \times \lambda} \quad (6)$$

$P_{clo,s,k}$  ( $k = 0, \dots, n$ ) are the saturated vapor pressures at each layer,  $kPa$ , calculated as eqn. (7). The temperature of each layer  $T_{clo,k}$  can be estimated as eqn. (8) <sup>45</sup>.  $T_{clo,0}$  is the skin (torso surface) temperature,  $35^\circ C$ .  $T_a$  is the environment temperature,  $20^\circ C$ .  $R_{ct}$  is the material intrinsic thermal resistance,  $^\circ C \cdot m^2 \cdot W^{-1}$ .  $R_{ct,bl}$  is the thermal resistance of the boundary layer,  $^\circ C \cdot m^2 \cdot W^{-1}$ ; due to the constant air velocity,  $R_{ct,bl}$  is constant. With greater  $w_{clo}$ ,  $R_{ct}(w_{clo})$  becomes lower and thus  $T_{clo,k}$  becomes greater. Thus,  $P_{clo,s,k}(w_{clo})$  increases with greater  $w_{clo}$ .  $P_a$  is the vapor pressure in the environment,  $kPa$ .

$$P_{clo,s,k} = \frac{e^{\frac{18.956 - 4030/(T_{clo,k} + 235)}{10}}}{10} \quad (7)$$

$$T_{clo,k} = T_{clo,0} - (T_{clo,0} - T_a) \times \frac{\frac{k}{n} \times R_{ct}(w_{clo})}{R_{ct}(w_{clo}) + R_{ct,bl}} \quad (8)$$

Therefore, the evaporation rate of the clothing system (eqn. (5)) can be re-written as eqn. (9). According to this equation, we hypothesized that  $\dot{m}_{evap}$  is positively related with  $w_{clo}$ . Similar to the concept of skin wettedness<sup>46</sup>,  $w_{clo}$  is the wettedness of clothed system (clothed wettedness). If a clothed human body contains a greater amount of water (i.e., it leads to a greater  $w_{clo}$ ), the clothed body has a higher evaporation rate<sup>2</sup>.

$$\dot{m}_{evap} = \sum_{k=0}^n A_{clo,k} w_k h_{m,k}(w_{clo}) (P_{clo,s,k}(w_{clo}) - P_a) \quad (9)$$

## 2.5 Statistical analyses

Statistical analyses were performed using the Statistical Package for the Social Sciences (SPSS) version 23.0 (IBM, Armonk, NY, USA). The individual effect of sweat rate and radiant heat on sweat transfer rates were analyzed by one-way analysis of variance (ANOVA) followed by Tukey's honestly significant difference (HSD, if the variance of the group was equal) or Tamhane's T2 (if the variance of the group was not equal) post-hoc tests for multiple comparison. The combined effects of sweat rate and material properties on evaporation rate were investigated with multiple linear regressions. The force enter method was chosen for predictor selection. The multicollinearity assessment, casewise diagnostics, assumptions of linearity and homoscedasticity and normality of residuals were also investigated for all the multiple linear regression models. The same method of multiple linear regressions was also performed between  $\dot{m}_{evap,P3}$  and  $\dot{m}_{evap,P2}$ .

## 3. Results and discussion

### 3.1 Effect of sweat rate on evaporation rate

Overall, the evaporation rate ( $\dot{m}_{evap}$ ) increased with the sweat rate ( $\dot{m}_{sweat}$ ) for both hydrophilic and hydrophobic materials (Fig. 4 (a-1) and (a-2)). The results agree with previous studies on nude subjects and subjects wearing swimming suits<sup>7, 47</sup>. The reason for the  $\dot{m}_{evap}$  increment could be the increased mean vapor pressure within the clothed Torso, which can also be explained by the increased clothed wettedness (eqn. (14)) caused by a higher sweat rate. The sweat evaporative efficiency ( $\eta_{evap}$ ) was inversely related to  $\dot{m}_{sweat}$  (Fig. 4 (b-1) and (b-2)). This demonstrates that, with higher sweat rate, less percentage of the sweat evaporates from a clothed system and the percentage of sweat accumulation and dripping increases. This could be explained by the relative permeability and saturation relationship<sup>48</sup>. With higher sweat rate, i.e., greater water saturation, the relative permeability of water vapor decreased, and the relative permeability of liquid water increased, which corresponds to the decreased percentage of sweat evaporation and higher percentage of sweat accumulation and dripping. The different slopes between the materials (Fig. 4) demonstrate that the effect of sweat rate on the evaporation rate and on the sweat evaporative efficiency also depend on material properties.

---

<sup>2</sup> Different environment conditions and active human body may influence the result of  $\dot{m}_{evap}$ . But since these are not the independent variables in the current research, we did not discuss these factors in this paper.



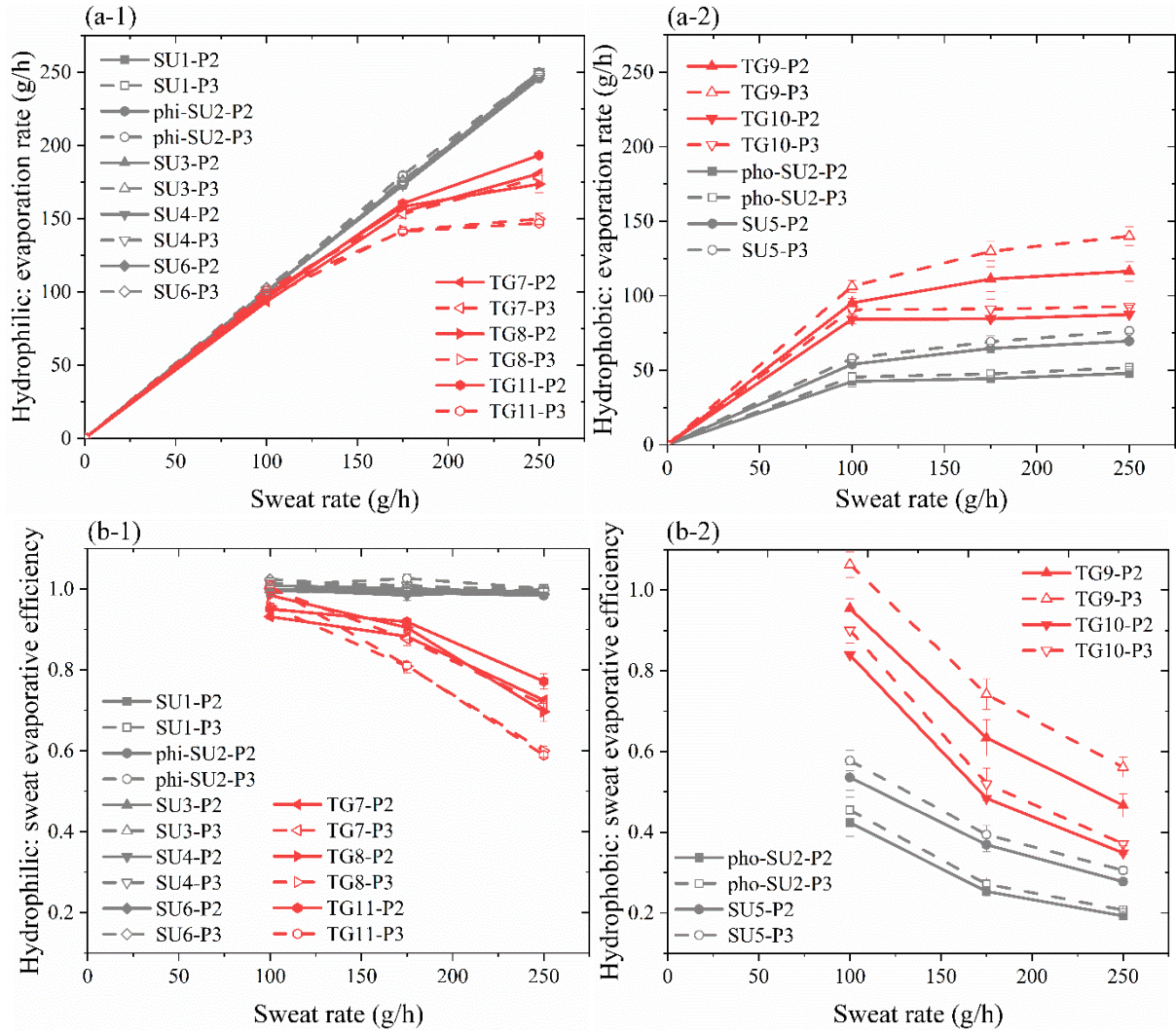


**Fig. 4 Relationship between evaporation rate and sweat rate for hydrophilic (a-1) and hydrophobic (a-2) materials. Relationship between sweat evaporative efficiency and sweat rate for hydrophilic (b-1) and hydrophobic (b-2) materials.**

### 3.2 Effect of material properties on evaporation rate

Table 2 presents the multiple linear regressions between the evaporation rate (P2:  $\dot{m}_{evap,P2}$ ; P3:  $\dot{m}_{evap,P3}$ ) and material properties. For SUs, material hydrophilicity/hydrophobicity showed a significant effect on  $\dot{m}_{evap,P2}$ ; for TGs, in addition to the significant effect of material hydrophilicity/hydrophobicity, material weight, thickness and evaporative resistance ( $R_{et}$ ) were also significant factors on  $\dot{m}_{evap,P2}$ . These material property effects are further discussed in 3.2.1 and 3.2.2.

In addition to the similar effects of material properties in P2, material emissivity showed a significant negative effect on  $\dot{m}_{evap,P3}$  for TGs. The reason could be that the low emissivity of material decreased the heat absorption from the external radiant heat source. The torso itself thus had to provide higher heating power to maintain the constant surface temperature<sup>49</sup>, which led to the higher evaporation rate.

**Table 2 Multiple linear regression between evaporation rate (P2:  $\dot{m}_{evap,P2}$ ; P3:  $\dot{m}_{evap,P3}$ ) and material properties for SUs and TGs.**

Material	R <sup>2</sup>	Factors	Unstandardized coefficient (a1-a7, b)	Standardized coefficient	Material	R <sup>2</sup>	Factors	Unstandardized coefficient (a1-a7, b)	Standardized coefficient
$\dot{m}_{evap,P2}$					$\dot{m}_{evap,P2}$				
SU	0.87	constant	62.39		TG	0.74	constant	-761.62	
		sweat rate **	0.36	0.42			sweat rate **	0.27	0.52
		hydrophilicity <sup>a</sup> **	-103.88	-0.89			hydrophilicity **	-61.97	-0.96
							weight *	1.94	2.9

				thickness *	-287.7	-6.2
				$R_{et}^b$ *	33.59	5.59
		$\dot{m}_{evap,P3}$				
	constant	-1.21		constant	135.56	
	sweat rate **	0.73	0.6	sweat rate **	0.28	0.63
0.89	hydrophilicity **	-126.69	-0.77	0.80	hydrophilicity **	-63.95
				weight *	0.11	0.19
				emissivity **	-99.97	-0.61

Note: The form of the regression equation is as follows:  $y = a_1 \cdot \text{sweat rate} + a_2 \cdot \text{hydrophilicity} + a_3 \cdot \text{weight} + a_4 \cdot \text{thickness} + a_5 \cdot R_{et} + a_6 \cdot R_{et} + a_7 \cdot \text{emissivity} + b$ ,  $y$  is the  $\dot{m}_{evap,P2}$  and  $\dot{m}_{evap,P3}$ , respectively. <sup>a</sup> If the material is hydrophilic, the value was labelled as 0; if the material is hydrophobic, the value was labelled as 1. <sup>b</sup>  $R_{et}$ : thermal resistance,  $R_{et}$ : evaporative resistance. \* $p < 0.05$ , \*\* $p < 0.001$ .

### 3.2.1 Relationship between evaporation rate and sweat accumulation ability

Fig. 5 demonstrates the significant positive relationship between the evaporation rate and the sweat accumulation ability ( $R^2 > 0.9$ ,  $p < 0.05$ ). This is in line with a previous human trial which demonstrated an increased evaporative mass loss with higher water content of clothing <sup>9</sup>. This could be explained by eqn. (9), the greater sweat accumulation, i.e., the higher clothed wettedness, leads to a greater evaporation rate <sup>7, 50</sup>.

We further investigated properties which potentially affect sweat accumulation ability (Fig. 5). Fig. 6a shows that hydrophilic materials accumulated more sweat than hydrophobic materials; multi-layered materials (TG) accumulated more sweat than single-layered materials (SU). Fig. 6b presents the positive relationship between the evaporative resistance and the sweat accumulation ability. The measurement of material evaporative resistance considered that the sweat evaporates on the skin and then the evaporated sweat transfers through the material. The greater evaporative resistance would decrease the sweat vapor transfer to the environment, leading a higher amount sweat accumulation within the clothing system. The measurement of evaporative resistance was conducted in an isothermal condition, i.e., no temperature gradient between environmental and skin temperature (35 °C). In our case, a lower environmental temperature (20 °C) compared to skin temperature (35 °C) possibly induces some condensation of vapor within the outer layer and, thus, further increasing the sweat accumulation amount. Fig. 6c-d showed the positive relationship between material weight and thickness and the sweat accumulation ability. It may be interesting to note that the weight and the thickness of TG showed opposite role in  $\dot{m}_{evap,P2}$ . The reason could be that even though greater weight and thickness may both lead to greater sweat accumulation, the greater thickness may hinder the evaporation due to the greater evaporation distance from the torso surface to the environment <sup>29</sup>, thus showing negative effect on the evaporation rate.

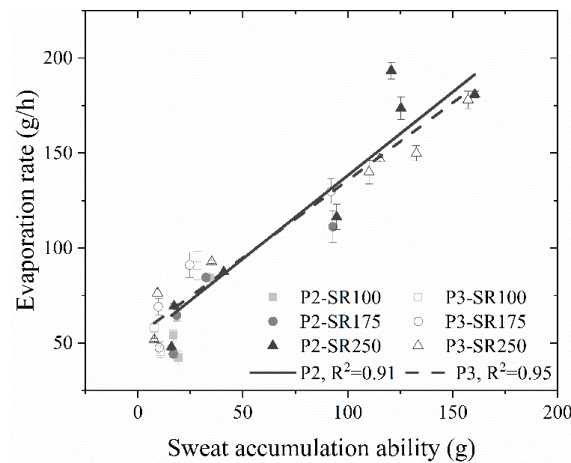
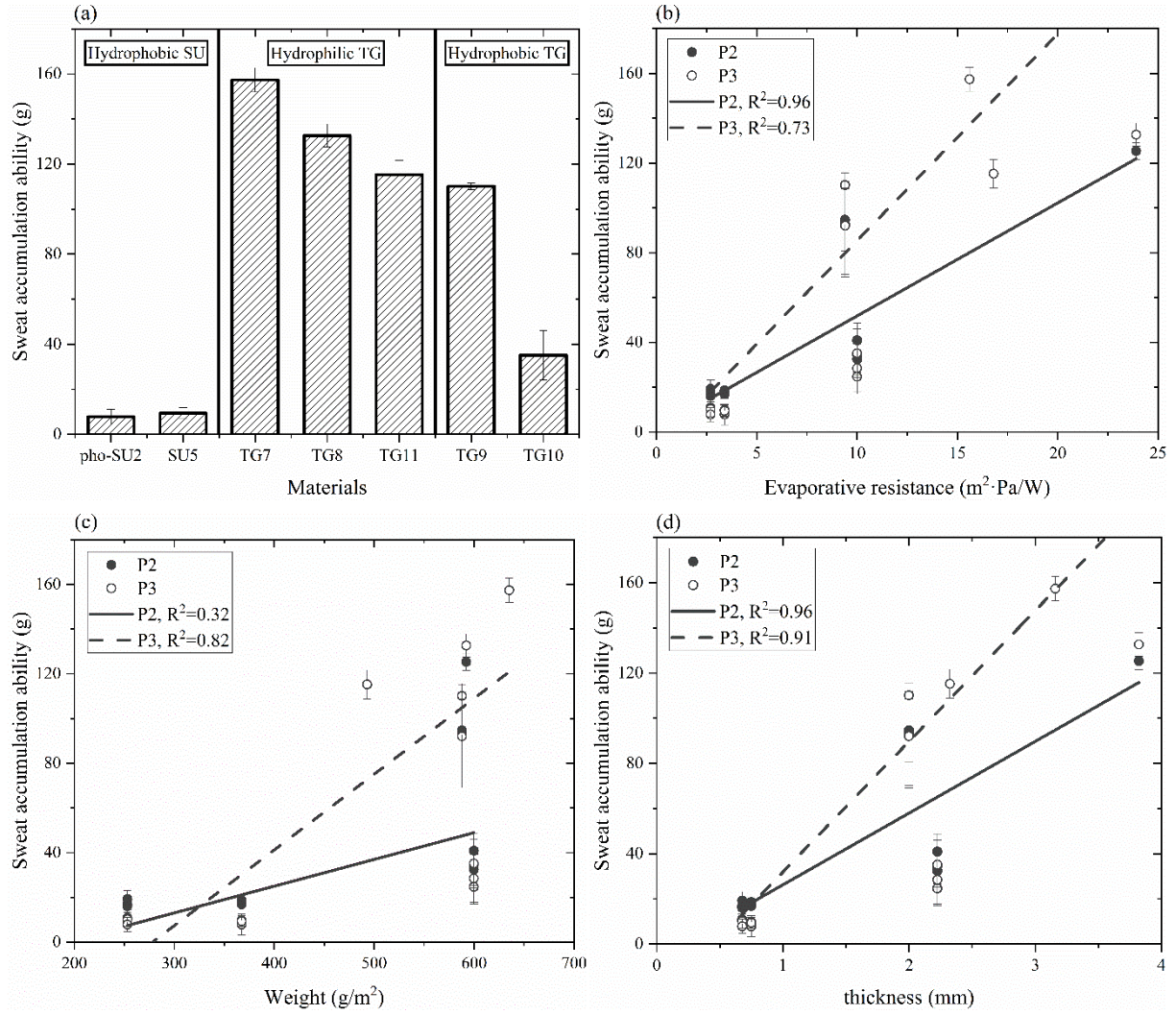


Fig. 5 Relationship between evaporation rate and sweat accumulation ability.



**Fig. 6 (a) Sweat accumulation ability of different material systems. Example: SR250 in P3. Since hydrophilic SUs did not reach moisture saturation, their sweat accumulation ability cannot be obtained. (b) Relationship between material evaporative resistance and sweat accumulation ability. (c) Relationship between material weight and sweat accumulation ability. (d) Relationship between material thickness and sweat accumulation ability.**

### 3.2.2 Relationship between evaporation rate and evaporative resistance

For hydrophilic materials,  $\dot{m}_{evap}$  of SUs was higher than that of TGs (Fig. 4 (a-1)). The explanation is that, the evaporative resistance ( $R_{et}$ ) of SUs is lower than that of TGs, leading to a higher mass transfer coefficient (eqn. (14)) and thus a higher evaporation rate. But for hydrophobic materials, SUs with lower  $R_{et}$  presented a lower  $\dot{m}_{evap}$  than TGs. To clarify the exact effect of evaporative resistance on the evaporation rate, the relationship between  $R_{et}$  and  $\dot{m}_{evap}$  was investigated (Fig. 7). The hydrophilic SUs (data points in dashed circles) evaporated all the sweat due to its high sweat accumulation ability. Except these cases, material  $R_{et}$  seems to show a dual relationship with evaporation rate. When  $R_{et}$  was low, it showed a positive relationship with  $\dot{m}_{evap}$ , which is opposite to the general understanding of evaporative resistance. The reason could be that the higher evaporative resistance corresponded to a higher sweat accumulation in the material (Fig. 6b), leading to a greater evaporation rate. But when  $R_{et}$  exceeded a certain value ( $\approx 20 \text{ m}^2 \cdot \text{Pa/W}$  in our cases),  $\dot{m}_{evap}$  tended to decrease with higher  $R_{et}$ . This may be due to the fact that evaporative resistance began to exert its negative effect in the evaporation process. For materials with high  $R_{et}$ , the material reached sweat saturation (i.e., the clothed wettedness was constant), thus the benefit of the sweat accumulation ability/clothed wettedness on the evaporation



rate remained constant. But higher  $R_{et}$  decreased the mass transfer coefficient  $h_{m,clo}$ , thus leading to a lower evaporation rate. This demonstrates the dual relationship of evaporative resistance with the evaporation process of the clothed system, different from the single negative impact which is commonly assumed.

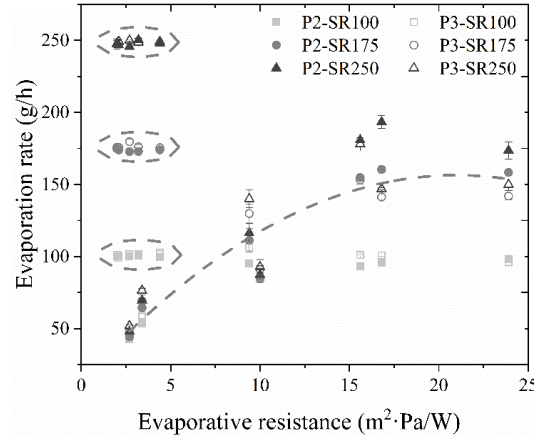


**Fig. 7 Relationship between evaporation rate and evaporative resistance.** Data points in black circle: hydrophilic SUs which can evaporate all the sweat (i.e.,  $\dot{m}_{evap} = \dot{m}_{sweat}$ ). The polynomial regression was performed for materials which cannot evaporate all the sweat, including hydrophobic SUs and all TGs. SR100-250: sweat rate 100, 175 and 250 g/h.

### 3.3 Effect of radiant heat on evaporation rate

Fig. 8 presents the comparison between the evaporation rate in P2 ( $\dot{m}_{evap,P2}$ ) and the evaporation rate in P3 ( $\dot{m}_{evap,P3}$ ). Table 3 presents the regression model of  $\dot{m}_{evap,P3}$  predicted by  $\dot{m}_{evap,P2}$  with  $R^2 = 0.824-0.999$ , showing that  $\dot{m}_{evap,P2}$  can account for more than 80 % of the variation in  $\dot{m}_{evap,P3}$ . The lower than 20 % of the variation that cannot be explained by  $\dot{m}_{evap,P2}$  demonstrates the difference between  $\dot{m}_{evap,P2}$  and  $\dot{m}_{evap,P3}$ .

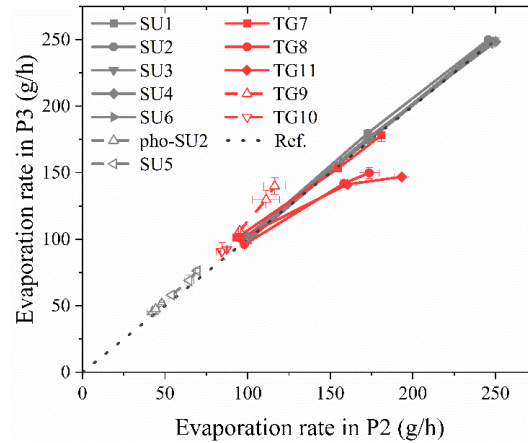


**Fig. 8 Comparison between the evaporation rate in P2 and P3 for all materials.** Solid line: hydrophilic materials; dash line: hydrophobic materials; dotted line: Ref., the reference line on which evaporation rate in P2 equals to that in P3.

**Table 3 Regression model of evaporation rate in P3 ( $\dot{m}_{evap,P3}$ ) predicted by evaporation rate in P2 ( $\dot{m}_{evap,P2}$ )**

Materials	Regression model	$R^2$	Sig.
SU	$\dot{m}_{evap,P3} = 0.990 * \dot{m}_{evap,P2} + 3.836$	0.999	$p < 0.001$
TG	$\dot{m}_{evap,P3} = 0.653 * \dot{m}_{evap,P2} + 41.765$	0.824	$p < 0.001$
SU and TG	$\dot{m}_{evap,P3} = 0.941 * \dot{m}_{evap,P2} + 8.542$	0.965	$p < 0.001$

Table 4 presents significant changes of  $\dot{m}_{evap}$  as well as  $\dot{m}_{accu}$  and  $\dot{m}_{drip}$  from P2 to P3 for different kinds of materials. Table 5 presents the magnitude of significant changes of  $\dot{m}_{evap}$ . For hydrophilic SUs, all the sweat evaporated in both P2 and P3 (i.e.,  $\dot{m}_{evap} = \dot{m}_{sweat}$ ,  $\dot{m}_{accu} = \dot{m}_{drip} = 0$ ). For hydrophilic TGs, at the low sweat rate 100 g/h, the radiant heat (P3) increased  $\dot{m}_{evap}$  (5.0 - 7.6 g/h, 5.2-8.2 %) and

decreased  $\dot{m}_{accu}$ ; at higher sweat rates 175 and 250 g/h, the radiant heat (P3) decreased  $\dot{m}_{evap}$  (16.3 - 46.4 g/h, 10.3-24.0 %) and increased  $\dot{m}_{drip}$ . For hydrophobic SUs and TGs, the radiant heat (P3) increased  $\dot{m}_{evap}$  (2.9 - 23.6 g/h, 6.1-20.3 %) and decreased  $\dot{m}_{drip}$  or  $\dot{m}_{accu}$ .

**Table 4 Change of sweat transfer rates from P2 to P3 for SUs and TGs**

Sweat transfer rate	Hydrophilic SUs	Hydrophilic TGs		Hydrophobic SUs/TG10	Hydrophobic TG9
		Low sweat rate (SR100)	High sweat rate (SR175/250)		
$\dot{m}_{evap}$	–	↑*	↓**	↑*	↑*
$\dot{m}_{accu}$	0	↓*	175g/h: –; 250g/h: ↓*	0	↓*
$\dot{m}_{drip}$	0	0	↑*	↓*	–

Note: “–”: there was no significant difference in sweat transfer rate between P2 and P3; “↑”: sweat transfer rate in P3 was significantly greater than that in P2; “↓”: sweat transfer rate in P3 was significantly lower than that in P2; “0”: there was no significant difference in sweat transfer rate from zero for both P2 and P3. \*p<0.05, \*\*p<0.01. SR100, SR175 and SR250: sweat rate 100, 175 and 250 g/h.

**Table 5 Change magnitude of evaporation rate from P2 to P3 ( $\Delta\dot{m}_{evap}=\dot{m}_{evap,P3}-\dot{m}_{evap,P2}$ ) for SU and TG**

Materials		SR100	SR175	SR250
Hydrophilic materials	TG7	7.6 (8.2 %)**	-1.5 (-1.0 %)	-2.9 (-1.6 %)
	TG8	-2.1 (-2.2 %)	-16.3 (-10.3 %)**	-23.7 (-13.7 %)**
	TG11	5.0 (5.2 %)*	-19.1 (-11.9 %)**	-46.4 (-24.0 %)**
Hydrophobic materials	pho-SU2	2.9 (6.9 %)*	3.2 (7.2 %)	3.8 (7.8 %)*
	SU5	4 (7.4 %)	4.5 (7.0 %)*	6.9 (9.9 %)*
	TG9	11.2 (11.8 %)*	18.6 (16.7 %)*	23.6 (20.3 %)**
	TG10	6.5 (7.7 %)	6.6 (7.8 %)	5.3 (6.1 %)*

Note: The percentage in the parentheses is the variation percentage from P2 to P3,  $(\dot{m}_{evap,P3} - \dot{m}_{evap,P2})/\dot{m}_{evap,P2}$ . \*p<0.05, \*\*p<0.01. SR100, SR175 and SR250: sweat rate 100, 175 and 250 g/h.

The MSR sensor measurements demonstrate that the radiant heat can increase the vapor pressure gradient from the Torso surface to the environment ( $p < 0.001$ ). This increased vapor pressure gradient could be the reason that the radiant heat increased evaporation rate in most cases. On the other hand, the possible explanation for the lower evaporation rate of hydrophilic TG8 and TG11 at higher sweat rates (175 and 250 g/h) is that when the temperature of the outer layers of TG is higher than that of the Torso surface, the larger amount of evaporated moisture will condense on the Torso surface and within the clothing layers, decreasing the evaporation rate. This hypothesis can be confirmed by our observations: (I) condensation on the Torso surface for TG8 and TG11 at higher sweat rates (Fig. 9 (a)); (II) condensation pattern that how liquid water distributed on the Torso surface followed the inner side structure of the material (Fig. 9 (b)). The inner sides of TG8 and TG11 have special structures which caused irregular contact between the material and the Torso surface and the condensation water thus formed at the position where the air space formed between the material and the Torso surface. The irregular air space may cause a higher temperature gradient between the Torso surface and the environment due to its high thermal resistance, facilitating the condensation. The special inner structures made TG8 and TG11 behave differently from other TGs. These observations give the picture that how sweat transfers from the human body through the clothing system. The sweat firstly evaporates on the skin surface, and part of the evaporated sweat may then condensates on the skin due to its lower temperature compared with the radiation environment. This condensation releases the heat to the skin and decreases the evaporation rate. It also accelerates the sweat accumulation and saturation of the clothed body, increasing the dripping rate. Furthermore, this evaporation-re-condensation process might be a steam burn mechanism caused by perspired moisture by condensation of sweat vapor and heat release.

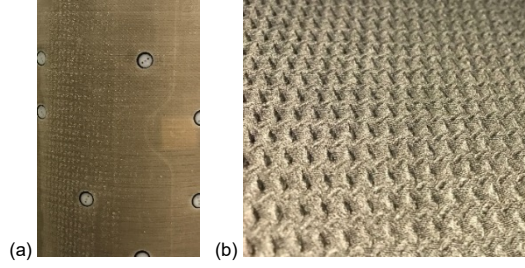


Fig.9 (a) Condensation pattern on the Torso surface in environment with radiant heat. (b) Material inside: special structure which produced irregular contact (air space) between the material and the Torso surface. Example: TG8.

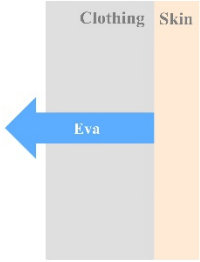
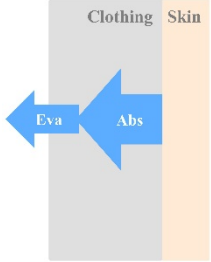
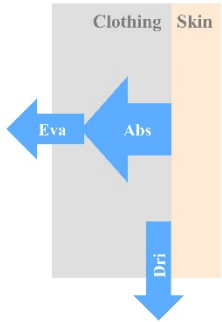
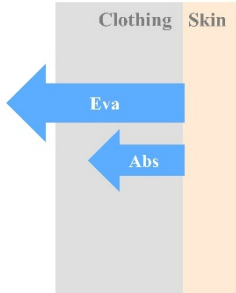
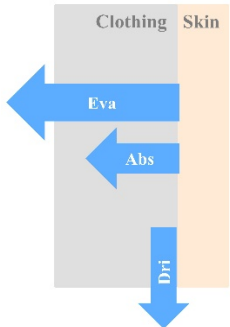
### 3.4 Dynamic sweat transfer process: combined analysis with evaporative cooling efficiency

The above results and discussion provide the knowledge of sweat transfer rates of clothed human body. Through combined analyses of the transfer rates and the apparent evaporative cooling efficiency ( $\eta_{cooling}$ )<sup>3 25</sup>, we can also get indications about the dynamic moisture transfer process. (I) As shown in a previous study<sup>51</sup>, four out of fifteen hydrophilic SU cases (five SUs at three sweat rates) with  $\eta_{cooling}$  lower than 1 ( $p < 0.05$ ) demonstrates that part of the sweat possibly evaporated from the clothing material. Meantime,  $\dot{m}_{accu}$  was zero for these cases. This demonstrates that the material absorbed the sweat and meanwhile evaporated the absorbed sweat under the same rate. (II) For other eleven SU cases and TG8 at sweat rate 100g/h,  $\dot{m}_{evap}$  equaled to  $\dot{m}_{sweat}$  and  $\eta_{cooling}$  equaled to 1. This demonstrates that all the sweat evaporated and all the evaporation possibly occurred on the Torso surface. (III) For TG8 at sweat rate 175 and 250 g/h and TG11 at 250 g/h,  $\eta_{cooling}$  was lower than 1 ( $p < 0.05$ ). Meantime, the sweat content in the material kept increasing ( $\dot{m}_{accu} > 0$ ,  $p < 0.01$ ), thus the sweat possibly evaporated within the material and the evaporation rate was lower than the absorption rate. (IV) For TG7 at three sweat rates and TG11 at sweat rate 100 and 175g/h,  $\eta_{cooling}$  was not lower than 1 ( $p < 0.05$ ) and  $\dot{m}_{accu} > 0$  ( $p < 0.05$ ). This demonstrates that part of sweat may evaporate on the Torso surface and part transferred to the material. The hypothesis of dynamic sweat transfer for hydrophilic SUs and TGs are summarized in Table 6.

Table 6 Dynamic sweat transfer process based on analyses of apparent evaporative cooling efficiency and sweat transfer rate

Category	Material cases	$\eta_{cooling}$	Sweat transfer rate	Dynamic process	Schematic diagram
I	4/15 SU cases	$< 1$	$\dot{m}_{evap} = \dot{m}_{sweat}$ , $\dot{m}_{accu} = 0$ , $\dot{m}_{drip} = 0$	The material absorbed all or part of the sweat and the absorbed sweat evaporated at the same rate.	

<sup>3</sup> Refer to literature [25] for the concept of apparent evaporative cooling efficiency ( $\eta_{cooling}$ ).  $\eta_{cooling} = E_{app}/(\dot{m}_{evap} * \lambda)$ .  $E_{app}$ : sweat cooling power (apparent evaporative heat loss),  $\dot{m}_{evap}$ : evaporation rate,  $\lambda$ : latent heat,  $\dot{m}_{evap} * \lambda$ : mass-based evaporative heat (evaporative cooling potential). Usually, if  $\eta_{cooling} \geq 1$ , all the sweat may evaporate on the skin; if  $\eta_{cooling} < 1$ , there may be sweat evaporating from the clothing layer.

II	10/15 SU cases; TG8, SR100	= 1	$\dot{m}_{evap} = \dot{m}_{sweat}, \dot{m}_{accu} = 0,$ $\dot{m}_{drip} = 0$	The material did not absorb the sweat, and all the sweat evaporated from the Torso surface.	
	TG8 (SR175)	< 1	$\dot{m}_{evap} < \dot{m}_{sweat}, \dot{m}_{accu} > 0,$ $\dot{m}_{drip} = 0$		
III	TG8 (SR250); TG11 (SR250)	< 1	$\dot{m}_{evap} < \dot{m}_{sweat}, \dot{m}_{accu} > 0,$ $\dot{m}_{drip} > 0$	Sweat evaporated within the material and the evaporation rate is lower than the absorption rate.	
	TG7 (SR100/175); TG11 (SR100/175)	> 1	$\dot{m}_{evap} < \dot{m}_{sweat}, \dot{m}_{accu} > 0,$ $\dot{m}_{drip} = 0$		
IV	TG7 (SR250)	= 1	$\dot{m}_{evap} < \dot{m}_{sweat}, \dot{m}_{accu} > 0,$ $\dot{m}_{drip} > 0$	Part of the sweat evaporated on the Torso surface and part transferred to the material.	

Note: In schematic diagrams, Eva, Abs and Dri refer to sweat evaporation, absorption and dripping, respectively. SR100, SR175 and SR250: sweat rate 100, 175 and 250 g/h.

#### 4. Conclusion

The study investigated the moisture transfer of clothed human body with continuous sweating under radiant heat exposure. Based on the novel findings, the concept of wettedness of clothed human body (clothed wettedness) in accordance to the concept of skin wettedness for nude human body, was proposed to better understand the evaporation process. Results showed that the evaporation rate of clothed body was increased with the sweat rate. The increment in evaporation rate was influenced by material properties (e.g., material composition, material hydrophilicity and evaporative resistance ( $R_{et}$ )) which affects sweat accumulation ability. Material evaporative resistance ( $R_{et}$ ) showed a dual relationship with the evaporation rate of clothed body. Evaporation rate was increased for greater  $R_{et}$  due to the higher moisture accumulation; when  $R_{et}$  exceeded a certain value, evaporation rate decreased with greater  $R_{et}$  due to the reduction in the mass transfer coefficient. A re-condensation of the evaporated sweat on the skin surface was also observed in radiant heat, leading to a reduction in the evaporation rate and an increase in the dripping rate. This evaporation-re-condensation phenomenon might lead to steam burn injuries in more hazardous conditions. The dynamic sweat transfer process was also investigated in detail by combined analyses of sweat transfer rate and apparent evaporative cooling efficiency. The findings from this study provide information for an in-depth understanding of sweat evaporation and its thermal effects for clothed human body in intensive physical exercises and environmental conditions including high radiation. Further study on exercising manikin/human body considering effect of movement as well as wind and air gap variation underneath the clothing may provide more realistic information on the sweat transfer process.

#### Conflict of interest

The authors declare that there is no conflict of interest.

#### Acknowledgements

The authors would like to thank DuPont, Switzerland and Trans–Textil, Germany for supplying the fabrics for this study and appreciate the technical support from Max Aeberhard, Ivo Rechsteiner and Shelley Kemp during the laboratory tests and the proofreading from Brit Maike Quandt. The authors would like to acknowledge the Fundamental Research Funds for the Central Universities (Grant NO. 2232018G-08), the financial support from the National Nature Science Foundation (Grant NO. 51576038), and Shanghai Municipal Natural Science Foundation (Grant NO. 17ZR1400500). The authors also gratefully acknowledge financial support from the China Scholarship Council.

#### Reference

1. Yin X, Chen Q and Pan N. A study and a design criterion for multilayer-structure in perspiration based infrared camouflage. *Experimental Thermal and Fluid Science*. 2013; 46: 211-20.
2. Mäkinen H, Smolander J and Vuorinen H. Simulation of the effect of moisture content in underwear and on the skin surface on steam burns of fire fighters. *Performance of Protective Clothing: Second Symposium*. ASTM International, 1988.
3. Barker RL, Guerth-Schacher C, Grimes RV and Hamouda H. Effects of Moisture on the Thermal Protective Performance of Firefighter Protective Clothing in Low-level Radiant Heat Exposures. *Textile Research Journal*. 2006; 76: 27-31.
4. Ghali K, Jones B and Tracy J. Modeling moisture transfer in fabrics. *Experimental thermal and fluid science*. 1994; 9: 330-6.



5. Fan JT, Cheng XY, Wen XH and Sun WW. An improved model of heat and moisture transfer with phase change and mobile condensates in fibrous insulation and comparison with experimental results. *International Journal of Heat and Mass Transfer*. 2004; 47: 2343-52.
6. Berglund LG and Gonzalez RR. Evaporation of sweat from sedentary man in humid environments. *J Appl Physiol Respir Environ Exerc Physiol*. 1977; 42: 767-72.
7. Candas V, Libert JP and Vogt JJ. Human skin wettedness and evaporative efficiency of sweating. *J Appl Physiol Respir Environ Exerc Physiol*. 1979; 46: 522-8.
8. Craig FN. Evaporative cooling of men in wet clothing. *J Appl Physiol*. 1972; 33: 331-6.
9. Craig FN and Moffitt JT. Efficiency of evaporative cooling from wet clothing. *J Appl Physiol*. 1974; 36: 313-6.
10. Hall JF. Effect of vapor pressure on physiologic strain and body heat storage. *J Appl Physiol*. 1963; 18: 808-11.
11. Nagata H. Evaporative heat loss and clothing. *J Hum Ergol (Tokyo)*. 1978; 7: 169-75.
12. Alber-Wallerstrom B and Holmer I. Efficiency of sweat evaporation in unacclimatized man working in a hot humid environment. *Eur J Appl Physiol Occup Physiol*. 1985; 54: 480-7.
13. Kondo N, Nishiyasu, T., & Ikegami, H. The influence of exercise intensity on sweating efficiency of the whole body in a mild thermal condition. *Ergonomics*. 1996; 39: 225-31.
14. Frye AJ and Kamon E. Sweating efficiency in acclimated men and women exercising in humid and dry heat. *J Appl Physiol Respir Environ Exerc Physiol*. 1983; 54: 972-7.
15. Candas V, Libert JP and Vogt JJ. Influence of air velocity and heat acclimation on human skin wettedness and sweating efficiency. *J Appl Physiol Respir Environ Exerc Physiol*. 1979; 47: 1194-200.
16. Givoni B. Elements of heat exchanges between man and his thermal environment. *Man, climate and architecture*. Applied Science Publishers, 1981.
17. Hettinger T. Belastung und Beanspruchung durch das Tragen persönlicher Schutzausrüstungen. Wirtschaftsverl. NW, 1985.
18. Vogt J, Candas V and Libert J. Graphical determination of heat tolerance limits. *Ergonomics*. 1982; 25: 285-94.
19. Vogt JJ, Candas V, Libert JP and Daull F. Chapter 6 Required Sweat Rate as an Index of Thermal Strain in Industry. In: Cena K and Clark JA, (eds.). *Studies in Environmental Science*. Elsevier, 1981, p. 99-110.
20. ASTM F1868 - 17, Standard Test Method for Thermal and Evaporative Resistance of Clothing Materials Using a Sweating Hot Plate. West Conshohocken, PA: ASTM International, 2017.
21. ASTM F2370 - 16, Standard Test Method for Measuring the Evaporative Resistance of Clothing Using a Sweating Manikin. West Conshohocken, PA: ASTM International, 2016.
22. ISO 11092:2014, Textiles -- Physiological effects -- Measurement of thermal and water- vapour resistance under steady-state conditions (sweating guarded-hotplate test). Geneva, Switzerland: International Organization for Standardization, 2014.
23. ISO 9920:2007, Ergonomics of the thermal environment -Estimation of thermal insulation and water vapour resistance of a clothing ensemble. Geneva, Switzerland: International Organization for Standardization, 2007.
24. ISO 7933:2004, Ergonomics of the thermal environment -- Analytical determination and interpretation of heat stress using calculation of the predicted heat strain. Geneva, Switzerland: International Organization for Standardization, 2004.
25. Havenith G, Richards MG, Wang X, et al. Apparent latent heat of evaporation from clothing: attenuation and "heat pipe" effects. *J Appl Physiol (1985)*. 2008; 104: 142-9.
26. Nish Y. Moisture permeation of clothing-A factor governing thermal equilibrium and comfort. *Ashrae Trans*. 1970; 76: 137.
27. Richards MG and Fiala D. Modelling fire-fighter responses to exercise and asymmetric infrared radiation using a dynamic multi-mode model of human physiology and results from the sweating agile thermal manikin. *Eur J Appl Physiol*. 2004; 92: 649-53.
28. Wang F, Annaheim S, Morrissey M and Rossi RM. Real evaporative cooling efficiency of one-layer tight-fitting sportswear in a hot environment. *Scand J Med Sci Sports*. 2014; 24: e129-39.
29. Havenith G, Brode P, den Hartog E, et al. Evaporative cooling: effective latent heat of evaporation in relation to evaporation distance from the skin. *J Appl Physiol (1985)*. 2013; 114: 778-85.
30. Cain B, & McLellan, T. M. A model of evaporation from the skin while wearing protective clothing. *International journal of biometeorology*. 1998; 41: 183-93.
31. Kwon A, Kato M, Kawamura H, Yanai Y and Tokura H. Physiological significance of hydrophilic and hydrophobic textile materials during intermittent exercise in humans under the influence of warm ambient temperature with and without wind. *European journal of applied physiology and occupational physiology*. 1998; 78: 487-93.
32. Brode P, Kuklane K, Candas V, et al. Heat gain from thermal radiation through protective clothing with different insulation, reflectivity and vapour permeability. *Int J Occup Saf Ergon*. 2010; 16: 231-44.
33. Keiser C and Rossi RM. Temperature Analysis for the Prediction of Steam Formation and Transfer in Multilayer Thermal Protective Clothing at Low Level Thermal Radiation. *Textile Research Journal*. 2008; 78: 1025-35.
34. Stämpfli R, Brühwiler PA, Rechsteiner I, Meyer VR and Rossi RM. X-ray tomographic investigation of water distribution in textiles under compression – Possibilities for data presentation. *Measurement*. 2013; 46: 1212-9.
35. Mosher H. Simultaneous study of constituents of urine and perspiration. *J Biol Chem*. 1933; 99: 781-90.
36. ISO18640-1:2018, Protective clothing for firefighters -- Physiological impact -- Part 1: Measurement of coupled heat and moisture transfer with the sweating torso. Geneva, Switzerland: International Organization for Standardization, 2018, p. 38.
37. ISO18640-2:2018, Protective clothing for firefighters -- Physiological impact -- Part 2: Determination of physiological heat load caused by protective clothing worn by firefighters. Geneva, Switzerland: International Organization for Standardization, 2018, p. 17.

38. Annaheim S, Wang L-C, Psikuta A, Morrissey MP, Camenzind MA and Rossi RM. A new method to assess the influence of textiles properties on human thermophysiology. Part I. *International Journal of Clothing Science and Technology*. 2015; 27: 272-82.
39. Zimmerli T and Weder MS. Protection and comfort—a sweating torso for the simultaneous measurement of protective and comfort properties of PPE. *Performance of protective clothing: Sixth Volume*. ASTM International, 1997, p. 271-80.
40. ISO 5084:1966, Textiles -- Determination of thickness of textiles and textile products. Geneva, Switzerland: International Organization for Standardization, 1996.
41. ISO 3801:1977, Textiles -- Woven fabrics -- Determination of mass per unit length and mass per unit area. Geneva, Switzerland: International Organization for Standardization, 1977.
42. ANSI/ASHRAE Standard 55-2017, Thermal Environmental Conditions for Human Occupancy. Atlanta, GA: ANSI/ASHRAE Standard, 2004.
43. Song G, Mandal S and Rossi RM. Fires and thermal environments. *Thermal Protective Clothing for Firefighters*. Cambridge: Woodhead Publishing, 2017, p. 8.
44. Wang F, Havenith G, Mayor TS, et al. Clothing real evaporative resistance determined by means of a sweating thermal manikin: a new round-robin study. *10th Manikin and Modelling Meeting (10i3m), Tampere, Finland*. 2014.
45. Wissler EH and Havenith G. A simple theoretical model of heat and moisture transport in multi-layer garments in cool ambient air. *Eur J Appl Physiol*. 2009; 105: 797-808.
46. Parsons KC and Ken P. *Human thermal environments : the effects of hot, moderate, and cold environments on human health, comfort, and performance*. Boca Raton: CRC Press, Taylor & Francis Group, 2014.
47. Tam HS, Darling RC, Downey JA and Cheh HY. Relationship between Evaporation Rate of Sweat and Mean Sweating Rate. *Journal of Applied Physiology*. 1976; 41: 777-80.
48. Li K and Horne RN. Comparison of methods to calculate relative permeability from capillary pressure in consolidated water-wet porous media. *Water resources research*. 2006; 42.
49. Guan M, Psikuta A, Camenzind M, et al. Effect of perspired moisture and material properties on evaporative cooling and thermal protection of the clothed human body exposed to radiant heat. *Textile Research Journal*. 0: 0040517518817067.
50. Gagge AP. A new physiological variable associated with sensible and insensible perspiration. 1937.
51. Guan M, Annaheim S, Li J, Camenzind M, Psikuta A and Rossi RM. Apparent evaporative cooling efficiency in clothing with continuous perspiration: A sweating manikin study. *International Journal of Thermal Sciences*. 2019; 137: 446-55.